SAN099-2408J

Draft 8/30/99 - To be submitted to J. Phys. Chemistry

Investigation of Sodium Distribution in Phosphate Glasses Using Spin-Echo ^{23}Na NMR[†]

Todd M. Alam,[1*] Jay Mclaughlin,[2‡¶] Carol C. Click,[3‡] Sam Conzone,[3‡]
Richard K. Brow, [3] Timothy J. Boyle[4] and Joe Zwanziger[2]

[1] Sandia National Laboratories, Department of Material Aging and Reliability, Albuquerque, NM 87185-1407 USA.
[2] Indiana University, Department of Chemistry, Bloomington, Indiana 47405 USA.
[3] University of Missouri-Rolla, Ceramic Engineering Department, Rolla, MO 65409-0330 USA.
[4] Sandia National Laboratories, Materials Processing Department, Advanced Materials Laboratory, 1001 University Blvd. SE., Albuquerque, NM 87106-1349 USA.

The spatial arrangement of sodium cations for a series of sodium phosphate glasses, xNa$_2$O·(100-x)P$_2$O$_5$ ($x < 55$), were investigated using ^{23}Na spin-echo NMR spectroscopy. The spin-echo decay rate is a function of the Na-Na homonuclear dipolar coupling and is related to the spatial proximity of neighboring Na nuclei. The spin-echo decay rate in these sodium phosphate glasses increases non-linearly with higher sodium number density, and thus provides a measure of the Na-Na extended range order. The results of these ^{23}Na NMR experiments are discussed within the context of several structural models, including a decimated crystal lattice model, cubic dilation lattice model, a hard sphere (HS) random distribution model and a pair-wise cluster hard sphere model. While the experimental ^{23}Na spin-echo M_2 are described adequately by both the decimated lattice and the random HS model, it is demonstrated that the slight non-linear behavior of M_2 as a function of sodium number density is more correctly described by the random distribution in the HS model. At low sodium number densities the experimental M_2 is inconsistent with models incorporating Na-Na clustering. The ability to distinguish between Na-Na clusters and non-clustered distributions becomes more difficult at higher sodium concentrations.

[†] Sandia is a multiprogram laboratory operated by Sandia Corporation, a Lockheed Martin Company, for the United States Department of Energy under Contract DE-AC04-94AL85000.
[*] Author to whom correspondence should be addressed.
[‡] Work partially performed as a participant of the student intern program at Sandia National Laboratories.
[¶] Present address: NIST, 100 Bureau Driver, MS 8562, Gaithersburg, MD 20899-8562.

DISCLAIMER

Introduction

The impact of different atomic constituents on the structure of glasses, and the resulting physical properties, continues to be an area of great interest. For simple oxide glasses the current structural paradigm suggests that these constituents are either network formers (i.e. P_2O_5, SiO_2 and B_2O_3), network modifiers (i.e. Li_2O, Na_2O, CaO) or intermediates (i.e. Al_2O_3).[1,2] The network formers produce well-defined coordination polyhedra that are linked into a three-dimensional network through bridging oxygens, while the network modifiers depolymerize this network through the formation of non-bridging oxygens. The intermediate components generally don't form glasses individually, but have network-like structures when combined with other network formers.

The large formal charge of +5 on phosphorous versus the +3 and +4 charges of boron and silicon results in distinct physical property and structural differences for these different glass systems. For example, an anomalous minimum in the glass transition temperature (T_g) and density (see Figure 1) is observed in alkali phosphate glasses,[3,4] whereas no corresponding behavior exists for the alkali silicate systems. In phosphate glasses this anomalous T_g and density behavior is attributed to the balance between the loss of the fully polymerized phosphate tetrahedral network with the initial addition of network modifiers (depolymerization) against the restructuring of the glass network due to the formation of oxygen-alkali bridges at higher modifier concentrations.[3,5,4] The changes in the glass structure due to the addition of network modifiers has been investigated using a wide variety of techniques, including nuclear magnetic resonance (NMR),[6,7,8 ,9-11,2] Raman,[12,4] and infrared (IR) spectroscopies,[3 ,12] X-ray and neutron diffraction,[13,5,14-16] and molecular dynamic (MD) simulations.[17,18] Unfortunately,

the impact of cation distribution on the restructuring of the glass and the presence of extended range cation order has not been completely addressed for alkali phosphate glass systems.

The role of cation distributions has been pursued in silicon and boron oxide glasses, where solid-state NMR investigations, including spin-echo, spin-echo double resonance (SEDOR) and rotational-echo double resonance (REDOR) techniques, have demonstrated that a wealth of information on modifier distribution can be obtained from these experiments. Spin-echo NMR experiments have been used to probe Na distribution in tellurite glasses,[19] along with the Na and Cs distributions in borate glasses.[20] The distribution of Al in sodium aluminoborate glasses has also been investigated using ^{11}B-^{27}Al REDOR experiments.[21] The structural impact of alkali distributions on the mixed alkali effect (MAE) in silicate glasses is perhaps the most extensively investigated area of cation distribution using NMR. In sodium silicate glasses, ^{23}Na spin-echo decay spectroscopy has been used to show that at low alkali content an inhomogeneous cation distribution is present,[22] which is consistent with molecular dynamic simulations of alkali silicate glasses.[23,24] For mixed alkali silicate glasses, ^{7}Li-^{23}Na SEDOR and ^{6}Li-^{23}Na SEDOR experiments,[25-27,22] along with ^{29}Si-^{23}Na and ^{29}Si-^{7}Li REDOR investigations have also been used to determine cation distribution.[22,28] From these NMR experiments Yap and co-workers[25] argued that preferential clustering of like cations was present in the Na-Li disilicate glass, in contrast to the conclusions of Eckert and co-workers[27,26,22,28] which showed no evidence for preferential interactions between unlike cations or preferential cation pairing.

While there has been numerous NMR investigations of cation distribution in silicate and borosilicate glasses, no comparable study of alkali phosphate glasses has been reported. In fact, while NMR has played a very important role in the investigation of the structure and dynamics

of the phosphate backbone,[6,7,29,9-11,30-32] details about the local environment of the network modifiers has been more limited. A ^{23}Na magic angle spinning (MAS) NMR investigation of the Na chemical shift in Li-Na metaphosphate glasses revealed that the Na and Li cations are uniformly mixed.[29] Recent ^{6}Li MAS NMR investigations of binary lithium ultraphosphate glasses demonstrate that the cation environment does not undergo any abrupt changes as a function of Li_2O concentration.[33] Wenslow and Mueller have used dynamic-angle-spinning (DAS) NMR experiments on mixed alkali glasses to demonstrate that there are multiple cation environments present.[34] Recently ^{23}Na-^{31}P cross-polarization (CP) MAS NMR experiments have demonstrated that the Na cation is associated with the fully polymerized phosphate tetrahedra in ultraphosphate glasses, presumably via coordination through terminal P=O bonds.[35] The question of cation clustering and segregation, or extended long-range order within phosphate glasses remains unanswered.

In this investigation we report the first ^{23}Na spin-echo decay NMR investigation to directly probe the Na-Na distribution for a series of sodium phosphate glasses. From these studies the resulting second moment (M_2), as a function of Na_2O modifier concentration, are related to the Na-Na distribution. These results for phosphate glasses are discussed in terms of various cation distribution models including random cation distribution as well as mutual cation clustering.

Fundamental Concepts and Methodology

The dephasing that occurs during a simple Hahn spin-echo pulse sequence, $90° - \tau - 180° - \tau - acquire$, can be used to access the strength of the homonuclear dipolar coupling between nuclei.[36] In spin-1/2 nuclei like ^{31}P, ^{15}N and ^{13}C the use of dipolar dephasing

experiments has become an important tool to probe distances in solids. For quadrupolar nuclei, (spin $I > 1/2$) structural information obtained from dipolar dephasing has seen limited development due to complications from first- and second-order quadrupolar perturbations and multiple transitions. Haase and Oldfield have shown that in the limit $H_Q^{(1)} >> H_{rf} >> H_D \approx H_Q^{(2)}$, (where H_{rf} is the interaction with the radio frequency pulse, H_D the dipolar interactions and $H_Q^{(1)}$ and $H_Q^{(2)}$ represent the first- and second-order quadrupolar interactions), the echo decay is Gaussian and allows the measurement of the average homonuclear dipolar second moment M_2:[37]

$$\frac{I(2\tau)}{I(0)} = \exp[-M_2(2\tau)^2/2] \qquad (1)$$

In Eqn. 1, $I(2\tau)$ represents the echo amplitude for the dephasing period τ, and $I(0)$ the echo amplitude for no dephasing. Following the formulation of van Vleck,[38] the spin-echo second moment is given by:

$$M_2 = \frac{9}{4} E_L^{(n)} \gamma^4 \hbar^2 \sum_{j<k} \frac{\left(1 - 3\cos^2 \theta_{jk}\right)^2}{r_{jk}^6} \qquad (2)$$

where γ is the gyromagnetic ratio of the nucleus of interest, r_{jk} is the distance between two different nuclei i and j, θ_{jk} is the angle between the internuclear vector and the applied magnetic field, and $E_L^{(n)}$ is a spin dependent factor defined by Haase and Oldfield.[37] The label $n =$

0,1,···[n<(I+1/2)] refers to the central transition and subsequent satellite transitions. By using selective π pulses, only terms corresponding to the central transition ($n = 0$) need to be considered in the evaluation of M_2. In addition, the use of a selective Hahn echo pulse sequence allows the second-order quadrupolar interactions that are present for ^{23}Na ($I = 3/2$) to be neglected.[37] Under these conditions Eqn. 2 for ^{23}Na can be rewritten as:[22,20]

$$M_2 = 0.9562\left(\frac{\mu_0}{4\pi}\right)^2 \gamma^4 \hbar^2 \sum_{j<k} r_{jk}^{-6} \tag{3}$$

Additional scaling factors have been presented in the case of strong heteronuclear dipolar coupling.[37] Experimentally, we have shown that the heteronuclear ^{23}Na-^{31}P dipolar coupling in these glasses is small and have a minimal impact on the measured M_2 values. Therefore these heteronuclear dipolar-scaling factors are not detailed here.

In amorphous materials it is often convenient to rewrite the explicit summation in Eqs. 2 and 3 in terms of the Na-Na pair distribution function, $g(r)$. As shown by Zwanziger and co-workers[19] the weighted contribution of the Na-Na dipolar term at each distance r can be replaced by $g(r)$ using the relation:

$$M_2 \propto \sum_{j<k} \frac{1}{r_{jk}^6} \rightarrow \int \frac{4\pi r^2 \rho_0 g(r)}{r^6} dr \tag{4}$$

This formulation of the second moment also allows the results from these types of NMR experiments to be incorporated into modeling efforts, including reverse Monte Carlo

investigations of glass structure and molecular dynamic simulations.[19,2] For the Monte Carlo models described in this paper, M_2 was calculated from *g(r)* using Eqn. 4.

Experimental Methods

Sample Preparation. The sodium glasses were prepared using a modification of the sealed ampoule technique previously described by Hudgens et al.[3] A sodium metaphosphate glass was prepared by melting crystalline $(NaPO_3)_6$ (Alfa Aesar) in a platinum crucible at 900 °C followed by rapid quenching onto stainless steel plates. The sodium metaphosphate glass was crushed and then combined with appropriate amounts of sublimed P_2O_5 for the ultraphosphate glass compositions. These mixtures were placed into sealed silica ampoules and heated to 900 °C. The hot ampoule was immediately placed under a nitrogen atmosphere for storage. The final compositions were analyzed by ^{31}P NMR, and were within 2% of the target composition. The glass densities were measured using Archemedis method (see Table 1 and Figure 1). The crystalline compounds $NaClO_4$ (Aldrich), $NaNO_3$ (Aldrich), $NaSO_4$ (Mallinckrodt), Na_2SO_3 (Aldrich), $NaPO_3$ (Aldrich) and NaC_2O_4 (J. T. Baker Chemical Co.) utilized in the M_2 calibration (described below), were used as received without further purification.

NMR Experiments. To measure the ^{23}Na second moment (M_2), a Hahn spin echo pulse sequence, $(90^\circ)_x - \tau - (180^\circ)_y - \tau$- *acquire*, with variable dephasing times (τ) was utilized. In general, the echo that forms at τ following the final 180° refocusing pulse decreases with increasing dephasing time due to homonuclear Na-Na dipole interactions, which are not refocused during the pulse sequence. Heteronuclear dipolar interactions are expected to be refocused in this sequence and therefore do not contribute to the echo decay. By measurement

of the resulting echo decay, the ^{23}Na M_2 was evaluated using Eqn. 1. The effect of ^{23}Na-^{31}P dipolar interactions on quenching the effectiveness of the ^{23}Na-^{23}Na homonuclear interaction was investigated by employing a 17 kHz ^{31}P decoupling field during the entire spin echo experiment on the $NaPO_3$ glass and crystal samples.

All spectra were obtained on a Bruker AMX400 at 162.0 and 105.9 MHz for ^{31}P and ^{23}Na respectively, using a 4mm MAS broadband probe. All experiments were performed at 298K unless otherwise noted. The ^{31}P MAS experiments for analysis of glass purity were obtained using a $\pi/2$ pulse of 3 - 4 μsec, a 12.5 kHz spinning speed, 16 scan averages with a 60s recycle delay. The ^{23}Na M_2 Hahn spin-echo experiments were obtained under static conditions, using a Bruker spherical MAS rotor insert kit to limit the sample volume to ~25% of the rotor volume and centered in the coil to minimize rf field inhomogeneity. The reduction of inhomogeneity effects has been shown to be important in these types of experiments.[19] The $^{23}Na\{^{31}P\}$ experiments were performed on a 4mm triple resonance probe employing a linear amplifier on the third channel for ^{31}P decoupling. A selective ^{23}Na $\pi/2$ pulse of $10 - 25$ μsec was used in conjunction with a 500 ms recycle delay, and 16 to 1024 signal averages. For each relaxation experiment 20 τ values were chosen, with the maximum interpulse delay corresponding to 20% intensity decay. For each glass composition, the M_2 spin-echo relaxation experiments were repeated 3-5 times, with the average M_2 values and standard deviations reported in Table 1. Moderate pulse powers were chosen to obtain maximum excitation of the central ^{23}Na transition, while attempting to minimize the excitation of the satellite transitions. To calibrate the experimentally determined M_2 with theoretically calculated values, 6 crystalline compounds were used to obtain the correlation:

$$M_2(calc) = 1.21 M_2(exp) + 0.09 \quad r^2 = 0.985 \qquad (5)$$

This correlation is very similar the ^{23}Na M_2 correlation previously reported for similar standard compounds.[19] Equation 5 was used to correct the experimental M_2 values (Table 1), and was taken into account in the interpretation of the discussion of M_2 values.

Monte Carlo Simulations. Monte Carlo simulations of a hard sphere (HS) liquid were performed using the reverse Monte Carlo (RMC) algorithm developed by McGreevy and Pusztai,[39] on a variety of Silicon Graphic platforms, including an Indy, O2 and Octane workstation. The radial potential, (r) for an HS liquid is given by:

$$U(r) = \begin{cases} \infty & r < \sigma \\ 0 & r > \sigma \end{cases} \qquad (6)$$

where σ is the cutoff radius of interest. Monte Carlo simulations were constructed using 10,000 atoms randomly placed in a box with dimensions determined by the sodium number density. The simulations were run using infinite boundary conditions, and each sodium atom was moved on average 10,000 times using a 0.04 Å step size. In order to assure that the simulations had converged, configurations were collected until the oscillations in the calculated M_2 were constant.

RMC simulations of the pair-wise cluster HS liquid were performed using similar conditions to those employed for the HS model described above. For the pair-wise cluster an additional coordination constraint was employed requiring the presence of a nearest neighbor Na within ±0.02 Å of the minimum σ cutoff distance for 95% of the Na atoms, while still

maintaining the correct average Na number density. This constraint gives rise to Na-Na pairs separated by σ as discussed below.

Results

The density and Na number density (ρ_{Na}) as a function of Na_2O modifier concentration for the phosphate glass series, $x Na_2O \cdot (100-x)P_2O_5$ ($5 \leq x \leq 55$), is shown in Figure 1 (see also Table 1). The experimental glass density shows a distinct minimum at approximately 20 mole % Na_2O. The variation of ρ_{Na} with modifier concentration is less dramatic, reflecting the changes in the relative weighting of the Na contribution to the overall density varies with composition. Even with these differences an inflection point at ~ 20 to 25 mole % Na_2O is observed in the ρ_{Na} behavior. Representative data for the ^{23}Na spin-echo experiment in the metaphosphate glass ($50Na_2O \cdot 50P_2O_5$) is shown in Figure 2. Deviation from a single Gaussian decay (solid line) as described in Eqn. 1 is evident at longer dephasing times (> 1ms). This deviation indicates that there are distributions in the Na-Na dipolar coupling strengths and that higher Na moments are influencing the spin-echo decay. At short dephasing evolutions, however, the spin-echo decay data is approximated well by a single Gaussian (Eqn. 1), as shown in the normalized logarithmic plot, where the first 20% of the decay is linear (inset Fig. 2). The slope of this logarithmic data is $-M_2/2$ allowing for determination of the ^{23}Na-^{23}Na second moment (M_2), which are given in Table 1 for the entire composition range investigated ($5 \leq x \leq 55$). Second moments were also determined for selected compositions at reduced temperatures to address the impact of ionic motion (Table 1). These data were indistinguishable from the results at ambient temperature, implying that ionic motion has a negligible impact on the ^{23}Na decay data. A slight decrease in

the linearity of the logarithmic correlation at reduced temperatures was observed for high Na_2O concentrations, but the resulting M_2 values were still indistinguishable within experimental error. To address the effects of ^{31}P-^{23}Na heteronuclear dipolar interactions on the ^{23}Na spin-echo decay, experiments utilizing ^{31}P decoupling were also performed (Table 1) and were found to have no effect on the measured ^{23}Na M_2 values and can be neglected during the M_2 analysis.

Discussion

For the sodium phosphate glasses investigated, $x Na_2O \cdot (100-x) P_2O_5$ ($5 \leq x \leq 55$), the observed ^{23}Na-^{23}Na M_2 values increase gradually with both Na_2O concentration and Na number density (ρ_{Na}), as shown in Figure 3a and 3b, respectively. With increasing Na_2O and ρ_{Na} the average distance between sodium atoms (r_{jk}) must decrease to satisfy density and compositional requirements, leading to an overall increase in the observed M_2 (Eqn. 3). There are several important qualitative observations that can be made. First, the M_2 data shows that there are no abrupt changes or variations in the Na-Na distribution as a function of Na_2O concentration or ρ_{Na}. In particular, there are no changes in the Na-Na distribution that correlate with the minimum in the T_g observed at the $20Na_2O \cdot 80P_2O_5$ composition.[3,4] The gradual increase in the ^{23}Na M_2 also suggests a relatively homogenous distribution of Na cations within the glasses, but a more detailed analysis is required to fully assess the possibility of Na cation-cation clustering in these phosphate glasses (see below). The second qualitative observation is that the variation of M_2 as a function of Na_2O concentration (Fig. 3a) shows a slightly larger non-linear behavior compared to the variation as a function of ρ_{Na} (Figure 3b). Recall that the variation of the overall density and ρ_{Na} as a function of Na_2O concentration is non-linear for this glass series (Table 1 and Figure 1). Because of the non-linear behavior, *some* of the changes

observed in the ^{23}Na M_2 as a function of Na_2O concentration result from simple changes in glass density. In the present investigation it is important that variations in the measured ^{23}Na M_2 values correlate with the Na-Na distribution, and *not* be a direct function of the overall glass density. Therefore, the ^{23}Na M_2 behavior is more accurately discussed as a function of ρ_{Na} (Figure 3b), and will be used throughout the remainder of the discussion on Na distribution. It should also be noted that by disconnecting variations in the ^{23}Na M_2 from changes in the overall glass density also precludes any correlation between the Na distribution and the observed minimum in the glass density.

Simulation of Sodium Cation Distribution. A full description of the Na cation distribution in the glass would require the determination of the complete Na-Na pair distribution function *g(r)*. Unfortunately, a direct evaluation of the Na-Na *g(r)* is not possible from NMR ^{23}Na M_2 data. M_2 is related to an integral over *g(r)* (Eqn. 4), but cannot be inverted to produce a unique solution to *g(r)*. Therefore, to extract information about the Na distribution from NMR M_2 measurements it is necessary to construct models of the Na distribution, calculate M_2, and then compare this result to experimental values. A given distribution model will provide a unique M_2 value, allowing a test of various models which can be discarded if the predicted and experimental M_2 values differ. These comparisons do not provide definitive proof of a given model; and one can only conclude that the distribution model is potentially correct. Thus, the M_2 NMR experiment provides a test for any model seeking to describe the sodium distribution in the glass, but does not in itself contain enough information to build a unique model.

Cubic Lattice and Decimated Crystal Lattice Models

The first two models investigated to describe the Na cation distribution in these sodium phosphate glasses represent limiting-case scenarios. The minimum M_2 value for a given sodium atom density can be established by using a cubic lattice model where the lattice size is adjusted to match the experimental sodium number density. The results are plotted in Figure 3 along with the experimentally measured ^{23}Na M_2 values. The cubic lattice model produces the lower limit for M_2 since the maximum distance between Na atoms at a given density is achieved by locating them in a cubic lattice. Maximizing the distance between atoms (for a fixed Na density), results in the minimum possible M_2 (see Eqn 3). The M_2 values for the cubic lattice model show a quadratic dependence as a function of ρ_{Na} because the model always results in the same sodium atom distribution (same number of Na atoms), differing only by the distance between Na atoms. The resulting second moment varies as $M_2 \sim r^{-6} \sim \rho^2$ (Eqn. 4), producing the quadratic increase in M_2 with respect to ρ_{Na}. This quadratic dependence is common for isotropically compressed models.[19] The cubic model predicts Na-Na distances between 4.0 Å for 50% Na_2O and 9.4 Å for the 5% Na_2O in order to obtain the desired number density. Note all of the experimental ^{23}Na M_2 values are well above the minimum predicted values in this cubic model (Figure 3).

To establish a reasonable upper limit on the ^{23}Na M_2 values, a decimated lattice model was constructed, based on the sodium atom distribution observed in crystalline $NaPO_3$ ($50\%Na_2O \cdot 50\%P_2O_5$).[40] By assuming the Na atoms closest approach within the phosphate glasses will be the same or larger than the closest Na-Na distance in the denser $NaPO_3$ crystal (~3.5 Å),[40] this model represents a reasonable upper limit for the observed ^{23}Na M_2 values. In the decimated lattice model the Na atoms are randomly removed from the $NaPO_3$ structure to

achieve the correct sodium number density. The predicted ^{23}Na M_2 values as a function of ρ_{Na} are plotted in Figure 3b. Figure 4a shows a representation of the Na distribution in the decimated lattice model at the 50% Na_2O composition. For the 20Å x 20Å x 20Å slice shown in Fig. 4a, only Na atoms are included because the ^{23}Na M_2 values result entirely from Na-Na homonuclear dipolar interactions. In Figure 4b the Na-Na pair correlation functions, *g(r),* at three different mole percentage Na_2O ($x = 10, 30, 50$) are presented. The pair correlation functions show clearly that there are no Na-Na interactions below r ~3.5 Å (i.e. $g(r) = 0$) as dictated by the $NaPO_3$ crystal structure used to build the model. Very distinct and periodic Na-Na spacings are observed for the decimated lattice structure *g(r)*, with the intensity decreasing as the Na number density is reduced due to the random decimation of the lattice. The decimated lattice model shows a linear correlation with ρ_{Na} ($M_2 \sim \rho$), because a fixed sodium-sodium distance is retained, while the occupancy of each site is determined by the sodium density. This linear behavior is markedly different from the quadratic behavior observed in the cubic lattice. The agreement between the experimental M_2 values and the decimated lattice model is reasonably good, with the experimental M_2 values slightly smaller than those predicted by the decimated lattice. This difference reflects the increase in disorder expected to occur in amorphous glasses in comparison to an ordered crystalline structure.

Since the cubic lattice and the decimated lattice models predict different functional forms of M_2, the experimental ^{23}Na M_2 data was fit to both linear and quadratic equations as a function of ρ_{Na} to help determine the functional dependence of the Na distribution. These results are shown in Figure 5. The quadratic relationship describes the variation of the experimental ^{23}Na M_2 as a function of ρ_{Na} only marginally better than a linear relationship, with the error in M_2 making a definitive separation difficult. The magnitude of the error observed in these ^{23}Na

M_2 spin-echo experiments is one of the major weaknesses in utilizing this NMR technique to access subtle changes in distributions.

While the cubic and decimated lattice models are useful for providing limits to the M_2 values, the models themselves are not compelling models for the real sodium atom distribution in amorphous systems. Isotropic compression models are not considered realistic since all the bonds must be compressed or lengthened as the Na density varies, which is an unlikely scenario. Variations in the bond length disorder between crystalline material and glasses is only a few percent and is unlikely a major structural feature of these glasses. The cubic lattice model is also a poor choice overall because it predicts an extremely ordered sodium atom distribution (cubic arrangement), which is highly unlikely to be found in the glasses. The decimated lattice model also describes an ordered system, but is unsatisfactory because the other constituents in the glass retain the same structure as $NaPO_3$, even at the high Na decimation levels required for other compositions. Recent MD simulations for lithium ultraphosphate glasses show that the alkali-alkali g(r) does not reveal the well ordered spacing as seen in Figure 4b, but instead predicts a *g(r)* that is very broad and featureless.[17] A more realistic description of glass structure should be obtained by utilizing Na distribution models that incorporate disorder for all the constituents. These random distribution models overcome some of the limitations of the cubic and decimated lattice models, and are described below.

Hard Sphere Liquid

As an example of modeling containing random Na distributions, a hard sphere (HS) Monte Carlo (MC) model utilizing a minimum Na-Na interaction distance σ (Eqn 6) were investigated. For these HS simulations, σ was varied between 3.0 and 4.0 Å to encompass the

experimental ^{23}Na M_2 values and result in a family of M_2 curves as a function of ρ_{Na} (shown in Figure 6). The resulting curves for the HS model are also non-linear with ρ_{Na}, with the degree of non-linearity becoming more prominent with increasing values of σ. The minimum approach distance of 3.0 Å is slightly larger then the minimum sodium-sodium distance of 2.8 Å seen in crystalline Na_2O.[41] These distances are significantly greater then the ionic radius of sodium atoms. Recall however, that in phosphate crystals and glasses, a coordination shell of oxygen atoms separates the sodium atoms. The average minimum approach distance which best fits the experimental data is 3.47 Å, which is very close to the 3.5 Å distance observed in the metaphosphate crystal ($NaPO_3$).

A 20Å x 20Å x 20Å slice of the HS model Na distribution, corresponding to the $50Na_2O \cdot 50\ P_2O_5$ glass with $\sigma = 3.1$ Å, is shown in Figure 7a. The Na-Na pair correlation functions for $xNa_2O \cdot (100\text{-}x)P_2O_5$ glasses ($x = 10,30,50$) are also shown in Fig. 7b. Similar to the decimated lattice model there are no Na-Na interactions for $r < \sigma = 3.1$ Å, (i.e. $g(r) = 0$). A maximum in $g(r)$ is observed for Na-Na distances near σ, but significant tailing and disorder are visible, with $g(r)$ reaching a constant value for $r > 5$ Å. The $g(r)$ maximum near σ becomes more pronounced at higher Na_2O concentrations and reflects the influence of a potential of mean force that occurs in HS models at higher number densities. Note that there are no direct Na-Na interaction potentials in this HS model. The general shape of the HS $g(r)$ (Fig. 7b) is very similar to the Li-Li $g(r)$ recently reported for MD simulations of lithium ultraphosphate glasses.[17] Because the measured M_2 is strongly controlled by very short Na-Na interactions via the r^{-6} dependence (see Eqn 3), those Na-Na pairs that are within $\sigma \pm 0.1$Å of each other are shown as bonded in Figure 7b, to visually help identify these close Na-Na interactions. It is interesting to note that while the

Na-Na cutoff distance is 3.1 Å, very few of the Na-Na interactions actually occur at this distance.

While there is significant scatter in the minimum Na-Na closest approach data (Figure 6), several important conclusions can still be made. First the general trend of the M_2 behavior with increasing ρ_{Na} can be explained using a simple HS model. This argues that the Na cations are randomly distributed within the glass system. Secondly, while the two minimum distances are very similar between the $NaPO_3$ crystal and the HS model, the actual cation distributions and predicted M_2 are very different because the decimated lattice model (Figure 4) represents an ordered system while the hard sphere model (Figure 7) describes a disordered system. Figure 6 also reveals that even though the ^{23}Na spin-echo experiment can probe M_2 at low sodium density concentrations (< 20%), the differences in the various σ curves become increasingly small at these concentrations. This similarity in the M_2 response for different σ results from the fact that in the HS models the ^{23}Na-^{23}Na interaction are expected to vanish as the Na density becomes very dilute. While this HS model may not be a unique model in describing a random Na distribution, it provides an easily evaluated estimate of the Na-Na nearest approach distance and can be used as a metric for future investigations of Na distributions in phosphate glasses.

Hard Sphere Cluster Models

Clustering of the alkali cations has been forwarded as a possible explanation for various physical properties observed in alkali containing phosphate glass systems. To address the question of Na-Na clustering in the sodium phosphate glasses discussed in this manuscript, a HS model containing distinct Na-Na pair-wise coordination constraints (i.e. containing Na-Na clusters) were investigated. Variation of the ^{23}Na M_2 as a function of ρ_{Na} for the HS cluster

model is shown in Figure 8, for different minimum cutoff distances σ, ranging from 3.1 Å to 3.9 Å. This family of M_2 curves is similar to that observed for the random HS model (Fig. 6), but deviates markedly at low Na_2O concentrations. For the cluster model the ^{23}Na M_2 does not approach zero in the limit of $\rho_{Na} \rightarrow 0$, but instead reaches a non-vanishing value related to the Na-Na distance in the pair-wise cluster via Eqn. 6. In figure 9a, a 20Å x 20Å x 20Å slice showing the Na distribution for the pair-wise cluster HS model in a $50Na_2O{\cdot}50P_2O_5$ glass with $\sigma = 3.1$ Å. In Fig. 9b the *g(r)* for the different glass compositions $xNa_2O{\cdot}(100\text{-}x)P_2O_5$ ($x = 10$, 30, 50) are shown. To aid in visualization, the Na-Na pairs that are $\sigma \pm 0.1$ Å are shown as bonded in Fig. 9a. Note the dramatic increased number of close Na-Na interaction (has shown by the depicted bonds) compared to the random HS model (Figure 7a). The increase in the number of close Na-Na interactions at $r \sim \sigma$ is also evident in *g(r)*, where the dominant feature of the Na-Na pair correlation function is a sharp peak at σ. The presence of Na-Na clustering is expected to lead to increased M_2 values. From a simplistic view, since there is a preference to form clusters, there will always be at least one Na as a next nearest neighbor for the entire range of Na_2O concentrations investigated, giving rise to a non-zero M_2 value (Eqn 6) even at low Na concentrations. The predicted ^{23}Na M_2 response for the cluster HS model deviates from that observed experimentally supporting the conclusion that the Na atoms do not cluster or segregate in these phosphate glasses, but instead are uniformly or randomly distributed. Larger size clusters would be expected to produce a similar response, with larger limiting M_2 values since there would be an increased number of close Na-Na interactions resulting in a faster decay.

The lack of Na clustering, especially at low Na_2O modifier concentrations, is consistent with the structural model developed by Hoppe for phosphate glasses.[13,5,14,15] In this model, the addition of Na_2O depolymerizes the fully condensed Q^3 phosphate tetrahedra to form Q^2

tetrahedra along with the creation of corresponding non-bridging oxygens (NBO). At low Na_2O concentrations, the Na atoms are isolated, coordinated by both NBO and double-bonded oxygens (DBO). This model predicts that there is a critical Na_2O mole fraction (x = 20-25%) at which all terminal oxygens are coordinated to Na. Above this critical modifier concentration the preferred isolation of the NaO_n polyhedron begins to disappear due to cation linking via shared edges and corners. The experimental observation of no Na-Na clustering at low Na_2O concentrations is consistent with the isolated Na cations predicted in the Hoppe structural model. The ability to monitor the change in the Na-Na environment above the predicted critical mole fraction ($x = 20 - 25\%$) in the experimental ^{23}Na M_2 values was also assessed. Unfortunately, the M_2 behavior for the random HS model (Fig. 6) and the HS pair-wise cluster model (Fig. 8) are very similar for $\rho_{Na} > 0.008$ $Å^{-3}$, corresponding to $x \sim 30\%$. This similarity in M_2 behavior makes it difficult to obtain definitive conclusions concerning the predictions of Hoppe's structural model at higher Na_2O concentrations.

Conclusions

These experiments demonstrate that ^{23}Na NMR spin-echo M_2 experiment can be used to efficiently investigate cation distribution in $x Na_2O \cdot (100-x) P_2O_5$ ($10 \leq x \leq 55$) glasses. The smooth, gradual increase in M_2 as a function of Na number density demonstrates that major variations in the Na-Na distribution does not directly influences the thermodynamic properties of the glass and does not correlate with the anomalous behavior of density or glass transition temperature. A variety of model distributions were evaluated and compared to the experimental M_2 values. The ^{23}Na M_2 results in these phosphate glasses are consistent with a Na-Na

distribution that is disordered in comparison to the distribution in crystalline systems, and can be described by a random HS model. This HS model predicts an average closest Na-Na approach distance of 3.47 Å, and a Na-Na pair correlation function that is very similar to the Li-Li pair correlation function recently reported in MD simulations.[17] A pair-wise Na-Na HS cluster model was found to predict M_2 values that deviated substantially from those observed experimentally, especially at low ρ_{Na} values. In conclusion, the spin-echo results for these Na phosphate glasses are consistent with a homogenous random distribution of Na atoms, with no evidence for Na-Na clustering. These ^{23}Na M_2 results provide an initial basis for future evaluations and comparisons of Na distribution in phosphate glasses, including Na distributions in mixed alkali systems, which are presently being pursued.

Acknowledgement

Sandia is a multiprogram laboratory operated by Sandia Corporation, a Lockheed Martin Company, for the United States Department of Energy under Contract DE-AC04-94AL85000.

References

(1) Paul, A. *Chemistry of Glasses*; Chapman and Hall: New York, 1990.

(2) Zwanziger, J. W. *Int. Review Phys. Chem.* **1998**, *17*, 65.

(3) Hudgens, J. J.; Martin, S. W. *J. Am. Ceram. Soc.* **1993**, *76*, 1691.

(4) Hudgens, J. J.; Brow, R. K.; Tallant, D. R.; Martin, S. W. *J. Non-Cryst. Solids* **1998**, *223*, 21.

(5) Hoppe, U. *J. Non-Cryst. Solids* **1996**, *195*, 138.

(6) Brow, R. K.; Kirpatrick, R. J.; Turner, G. L. *J. Non-Cryst. Solids* **1990**, *116*, 39.

(7) Brow, R. K.; Phifer, C. C.; Turner, G. L.; Kirkpatrick, R. J. *J. Am. Ceram. Soc.* **1991**, *74*, 1287.

(8) Eckert, H. *Progress in NMR Spectroscopy* **1992**, *24*, 159.

(9) Brow, R. K.; Kirkpatrick, R. J.; Turner, G. L. *J. Amer. Ceramic Society* **1993**, *76*, 919.

(10) Brow, R. K.; Tallant, D. R.; Hudgens, J. J.; Martin, S. W.; Irwin, A. D. *J. of Non-Crystalline Solids* **1994**, *177*, 221.

(11) Kirkpatrick, R. J.; Brow, R. K. *Solid State Nuclear Magnetic Resonance* **1995**, *5*, 9.

(12) Meyer, K. *J. Non-Cryst. Solids* **1997**, *209*, 227.

(13) Hoppe, U.; Walter, G.; Kranold, R.; Stachel, D.; Barz, A. *J. Non-Cryst. Solids* **1995**, *192&193*, 28.

(14) Hoppe, U.; Walter, G.; Kranold, R.; Stachel, D.; Barz, A.; Hannon, A. C. *Physica B.* **1997**, *234-236*, 388.

(15) Hoppe, U.; Walter, G.; Stachel, D.; Barz, A.; Hannon, A. C. *Z. Naturforsch.* **1997**, *52a*, 259.

(16) Kranold, R.; Walter, G.; Lembke, U.; Rieker, T.; Stachel, D. *J. Non-Cryst. Solids* **1998**, *232-234*, 502.

(17) Liang, J.-J.; Cygan, R. T.; Alam, T. M. *J. Non-Cryst. Solids* **1999**, (In Press).

(18) Speghini, A.; Sourial, E.; Peres, T.; Pinna, G.; Bettinelli, M.; Capobianco, J. A. *Phys. Chem. Chem. Phys.* **1999**, *1*, 173.

(19) Zwanziger, J. W.; McLaughlin, J. C.; Tagg, S. L. *Phys. Rev. B* **1997**, *56*, 5243.

(20) Ratai, E.; Janssen, M.; Eckert, H. *Solid State Ionics* **1998**, *105*, 25.

(21) Wüllen, L. V.; Züchner, L.; Müller-Warmuth, W.; Eckert, H. *Solid State Nuclear Magnetic Resonance* **1996**, *6*, 203.

(22) Wüllen, L. V.; Gee, B.; Züchner, L.; Bertmer, M.; Eckert, H. *Ber. Bunsenges. Phys. Chem.* **1996**, *100*, 1539.

(23) Huang, C.; Cormack, A. N. *J. Chem. Phys.* **1990**, *93*, 8180.

(24) Huang, C.; Cormack, A. N. *J. Chem. Phys.* **1991**, *95*, 3634.

(25) Yap, A. T.-W.; Forster, H.; Elliot, S. R. *Phys. Rev. Lett.* **1995**, *75*, 3956.

(26) Gee, B.; Eckert, H. *Ber. Bunsenges. Phys. Chem.* **1996**, *100*, 1610.

(27) Gee, B.; Eckert, H. *J. Phys. Chem.* **1996**, *100*, 3705.

(28) Gee, B.; Janssen, M.; Eckert, H. *J. Non-Cryst. Solids* **1997**, *215*, 41.

(29) Sato, R. K.; Kirkpatrick, R. J.; Brow, R. K. *J. Non-Crystalline Solids* **1992**, *143*, 257.

(30) Rufflé, B.; Beaufils, S.; Gallier, J. *Chem. Phys.* **1995**, *195*, 339.

(31) Hartman, P.; Vogel, J.; Jäger, C. *Ber. Bunsenges. Phys. Chem.* **1996**, *100*, 1658.

(32) Alam, T. M.; Brow, R. K. *J. Non-Crystalline Solids* **1998**, *223*, 1.

(33) Alam, T. M.; Conzone, S.; Brow, R. K.; Boyle, T. J. *J. Non-Cryst. Solids* **1999**.

(34) Wenslow, R. M.; Mueller, K. T. *J. Non-Cryst. Solids* **1998**, *231*, 78.

(35) Prabakar, S.; Wenslow, R. M.; Mueller, K. T. *J. Non-Cryst. Solids* **1999**.

(36) Engelsberg, M.; Norberg, R. E. *Phys. Rev. B* **1972**, *5*, 3395.

(37) Haase, J.; Oldfield, E. *J. Magn. Reson., Ser. A* **1993**, *101*, 30.

(38) van Vleck, J. H. *Phys. Rev.* **1948**, *74*, 1168.

(39) McGreevy, R. L.; Pusztai, L. *Molecular Simulations* **1988**, *1*, 359.

(40) McAdam, A.; Jost, K. H.; Beagley, B. *Acta Cryst.* **1968**, *B24*, 1621.

(41) Mazurin, O. V.; Streltsina, M. V.; Shvairkovskaja, T. P. *Handbook of Glass Data, Part A*; Elsevier: New York, 1983.

TABLE 1: Average ^{23}Na-^{23}Na Second Moment M_2 Determined for Sodium Phosphate Glasses Using ^{23}Na Spin Echo Experiments

Glass Composition[a]				^{23}Na spin echo M_2^{Na-Na} (10^6 rad^2/s^2) [b]	
Batch	Actual	Density (g/cm^3)	Na # Density (Å^{-3}) 10^{-3}	Experiment[c]	Corrected[d]
$5Na_2O{\cdot}95P_2O_5$	$6.0Na_2O{\cdot}94.0P_2O_5$	2.438	1.06	0.31 ± 0.01 (0.30 ± 0.01)[e] (0.31 ± 0.01)[f]	0.47 ± 0.02 (0.46 ± 0.02)[e] (0.47 ± 0.02)[f]
$10Na_2O{\cdot}90P_2O_5$	$10.1Na_2O{\cdot}89.9P_2O_5$	2.432	2.19	0.690 ± 0.17	0.93 ± 0.22
$15Na_2O{\cdot}85P_2O_5$	$16.4Na_2O{\cdot}83.6P_2O_5$	2.414	3.36	0.72 ± 0.01	0.97 ± 0.01
$20Na_2O{\cdot}25P_2O_5$	$19.3Na_2O{\cdot}80.7P_2O_5$	2.385	4.56	1.35 ± 0.19	1.73 ± 0.24
$25Na_2O{\cdot}75P_2O_5$	$25.4Na_2O{\cdot}74.6P_2O_5$	2.397	5.92	1.99 ± 0.11	2.51 ± 0.14
$30Na_2O{\cdot}70P_2O_5$	$28.6Na_2O{\cdot}71.4P_2O_5$	2.418	7.40	2.28 ± 0.31	2.86 ± 0.39
$35Na_2O{\cdot}65P_2O_5$	$34.5\ Na_2O{\cdot}65.5\ P_2O_5$	2.442	9.03	2.44 ± 0.32	3.06 ± 0.40
$40Na_2O{\cdot}60P_2O_5$	$40.0Na_2O{\cdot}60.0P_2O_5$	2.480	10.86	3.82 ± 0.32	4.73 ± 0.40
$45Na_2O{\cdot}55P_2O_5$	$43.0\ Na_2O{\cdot}57.0\ P_2O_5$	2.488	12.73	4.40 ± 0.74	5.44 ± 0.91
$50Na_2O{\cdot}50P_2O_5$	$51.5Na_2O{\cdot}48.5P_2O_5$	2.508	14.86	5.25 ± 0.42 (4.9 ± 0.50)[e] (5.15 ± 0.4)[f]	6.47 ± 0.52 (6.02 ± 0.61)[e] (6.35 ± 0.49)[f]
$55Na_2O{\cdot}45P_2O_5$	$54.8\ Na_2O{\cdot}45.2\ P_2O_5$	2.534	17.05	7.02 ± 0.97	8.62 ± 1.19

[a] Composition as batched and as determined from integration of Q^n phosphate tetrahedron using ^{31}P MAS NMR and the relationship $f_{Q^2} = x/(100-x)$, $f_{Q^3} = 1 - f_{Q^2}$ for $0 < x < 50$, as described in Ref. 11. [b] Error in M_2 estimated from standard deviation of multiple experiments. [c] M_2 values experimentally determined from decay of ^{23}Na spin echo at 298K. [d] Corrected M_2 values based on crystal calibration as described in experimental section using Eqn 5. [e] M_2 values obtained at 173K. [f] M_2 values obtained under the presence of ^{31}P decoupling.

Figures

Figure 1 Variation of the glass density (●) and sodium number density, ρ_{Na} (○) with Na_2O mole fraction in the $xNa_2O{\cdot}(100\text{-}x)P_2O_5$ glass series. A minimum in the density was observed near $x \sim$ 20-25%, while ρ_{Na} shows a variation in slope at the same Na_2O concentration.

Figure 2 ^{23}Na spin echo NMR data (●) as a function of dephasing times τ for vitreous sodium metaphosphate ($50Na_2O{\cdot}50P_2O_5$). A strong deviation from a theoretical single Gaussian decay (———) is observed at longer τ delays. The initial 20% of the spin-echo decay is approximated well by a Gaussian as seen in the normalized logarithmic plot of spin-echo decays (inset). The slope of this data is $-M_2/2$ (Eqn. 1) where M_2 is the homonuclear ^{23}Na-^{23}Na second moment.

Figure 3 Experimental ^{23}Na spin echo second moment M_2 values (●) for the $xNa_2O{\cdot}(100\text{-}x)P_2O_5$ glass series as a function of a) Na_2O mole fraction and b) sodium number density, ρ(Na). Predicted theoretical M_2 values for the cubic dilation lattice model (————) and the decimated lattice model (- - - - -) are also shown. Details about the theoretical models are given in the text.

Figure 4 Representation of the sodium distribution in the decimated crystal lattice model based on the crystal structure of $NaPO_3$: a) a molecular picture (20 Å x 20 Å x 20 Å slice) showing only the Na atoms, b) the pair correlation function, *g(r)* for the decimated lattice model in the $xNa_2O{\cdot}(100\text{-}x)P_2O_5$ glasses, x = 10,30 50. The *g(r)* baselines are offset for clarity. Note the well order lattice spacing between Na atoms for this model.

Figure 5 Experimental ^{23}Na spin echo second moments M_2 for the sodium phosphate glasses with best fits to linear and quadratic increases in M_2 as a function of sodium number density $\rho(Na)$.

Figure 6. Theoretical set of M_2 curves for the Hard Sphere (HS) model. Curves for different minimum Na-Na distances (σ), 3.0, 3.2, 3.4, 3.6, 3.8 and 4.0 Å are shown. The experimental M_2 values (●) are shown for comparison.

Figure 7 Representation of sodium distribution for a random hard sphere (HS) liquid model: a) a molecular picture (20 Å x 20 Å x 20 Å slice) of the HS model for a Na-Na cutoff distance of $\sigma = 3.1$ Å, b) the Na-Na pair correlation function, *g(r)* for the random HS model in the $x Na_2O{\cdot}(100\text{-}x)P_2O_5$ glasses, $x = 10,30\ 50$, with $\sigma = 3.1$ Å. In (a) bonds are shown for those Na atoms that are at $\sigma \pm 0.1$ Å, while in (b) the *g(r)* are offset for clarity. Note that there is a very broad distribution of Na-Na distances that occur above the σ value, with very little ordering even at $x = 50$ concentrations.

Figure 8 Theoretical set of M_2 curves for the Hard Sphere model involving Na-Na pair clustering. Curves for different minimum Na-Na distances (σ), 3.1, 3.3, 3.5, 3.7 and 3.9 Å are shown. The experimental M_2 values (●) are shown for comparison. Note that the limiting M_2 value at low Na number density ($\rho_{Na} \rightarrow 0$) is nonzero.

Figure 9 Representation of sodium distribution for a hard sphere (HS) liquid model with Na-Na pair wise clusters: a) a molecular picture (20 Å x 20 Å x 20 Å slice) of the HS cluster model for

a Na-Na cutoff distance of $\sigma = 3.1$ Å. b) the pair correlation function, *g(r)* for the HS cluster model in the $x Na_2O \cdot (100-x)P_2O_5$ glasses, $x = 10,30\ 50$ and $\sigma = 3.1$ Å. In (a) bonds are shown for those Na atoms that are at $\sigma \pm 0.1$ Å, while in (b) the *g(r)* are offset for clarity. Note that there is a very sharp peak of Na-Na distances at the σ value, indicating that almost all of the Na atoms occur as Na-Na pairs or clusters.

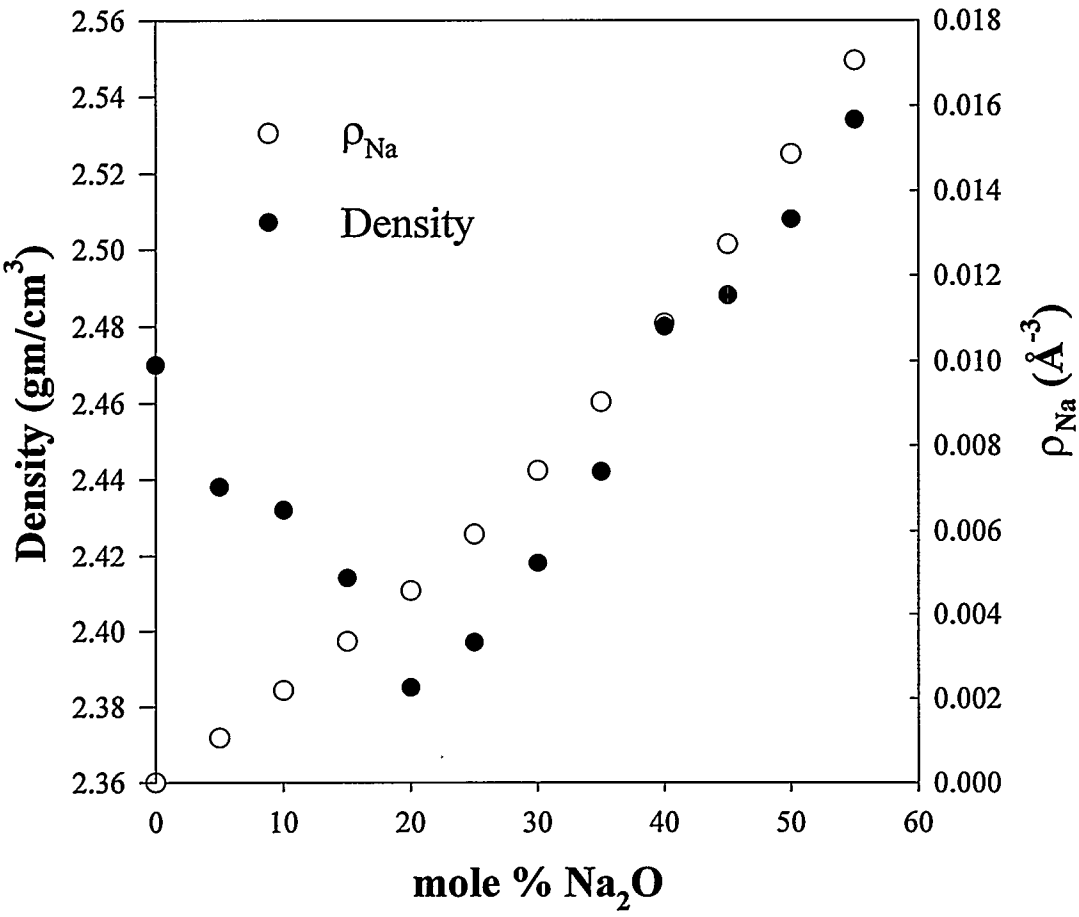

Alam et al. Fig. 1

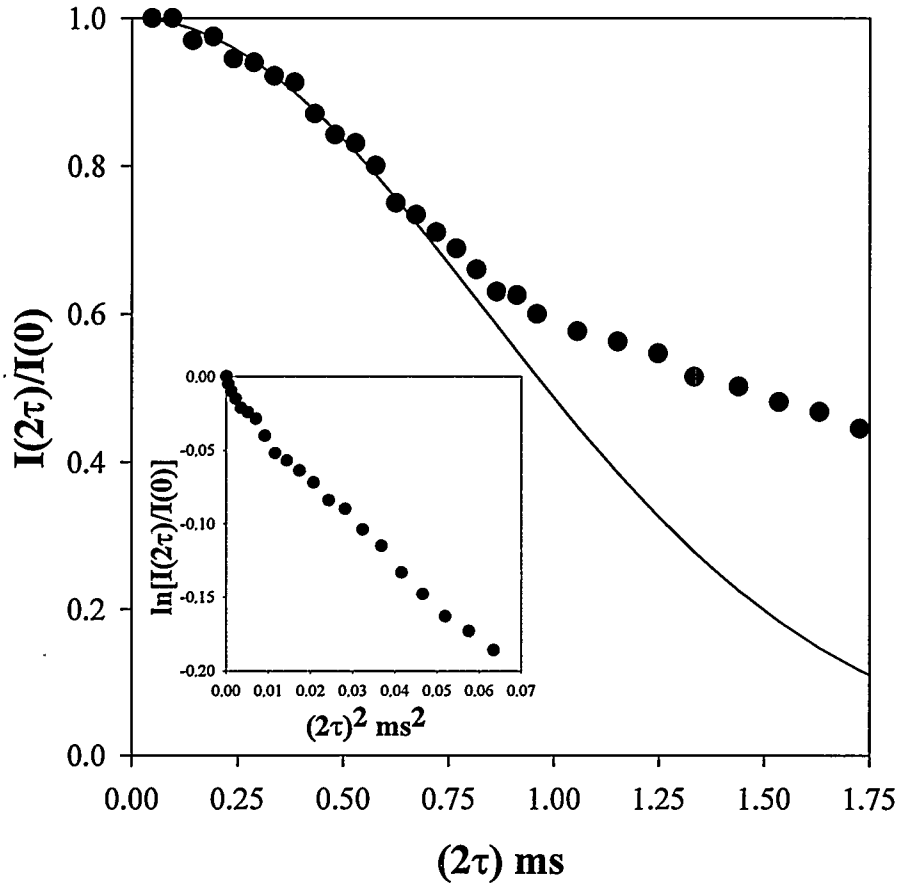

Alam et al. Fig. 2

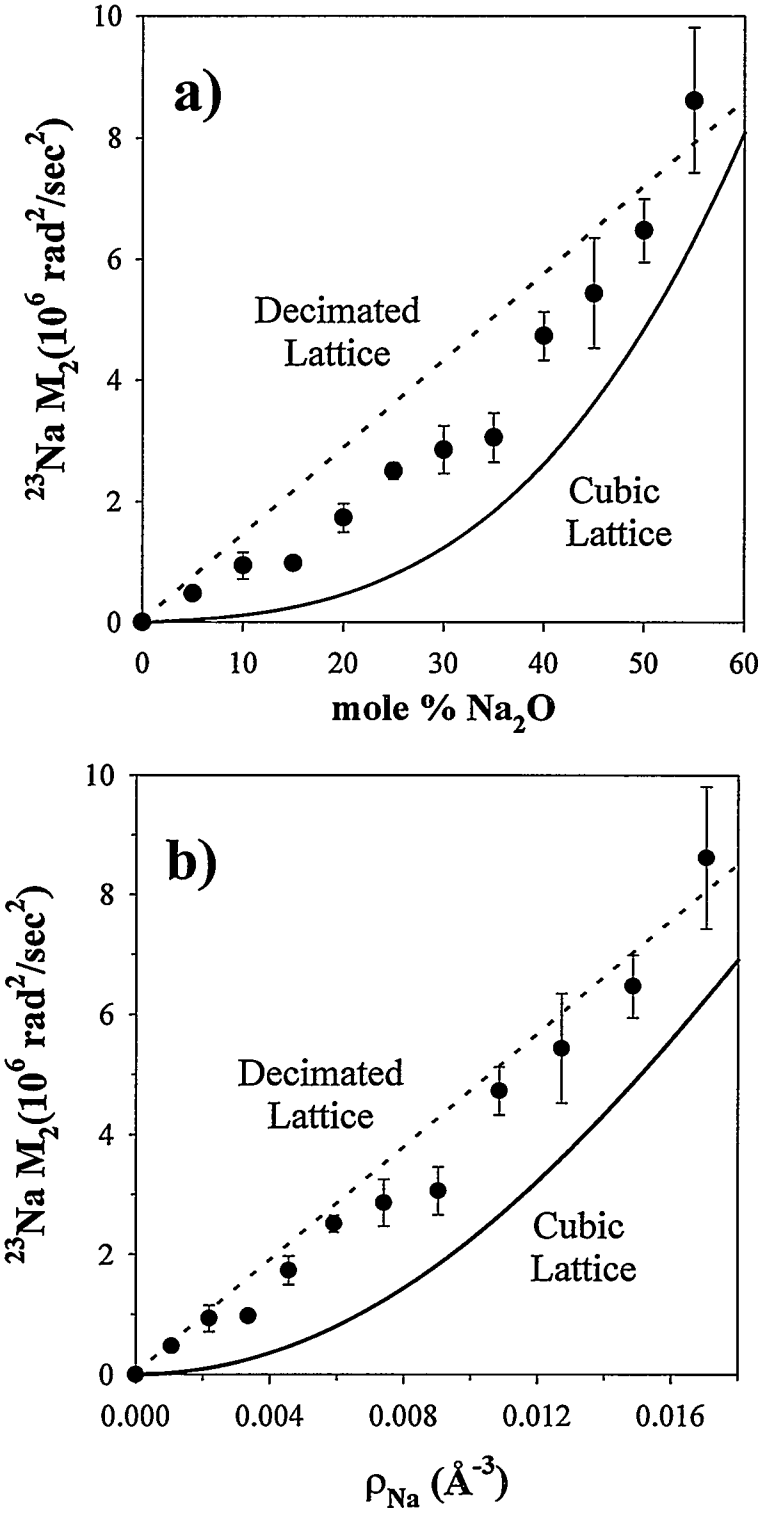

Alam et al. Fig. 3

a)

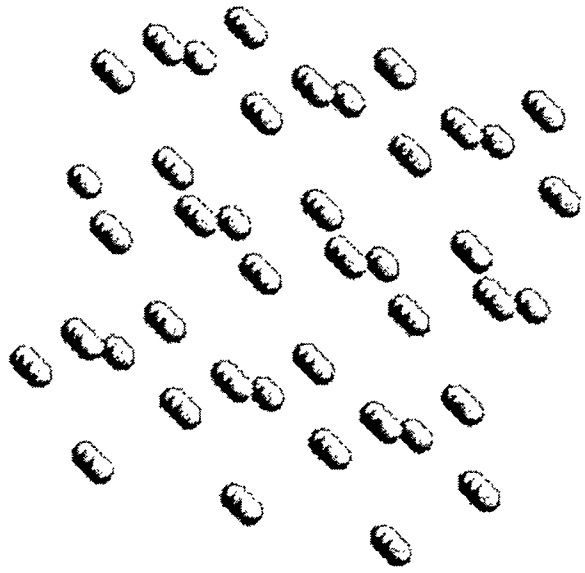

b)

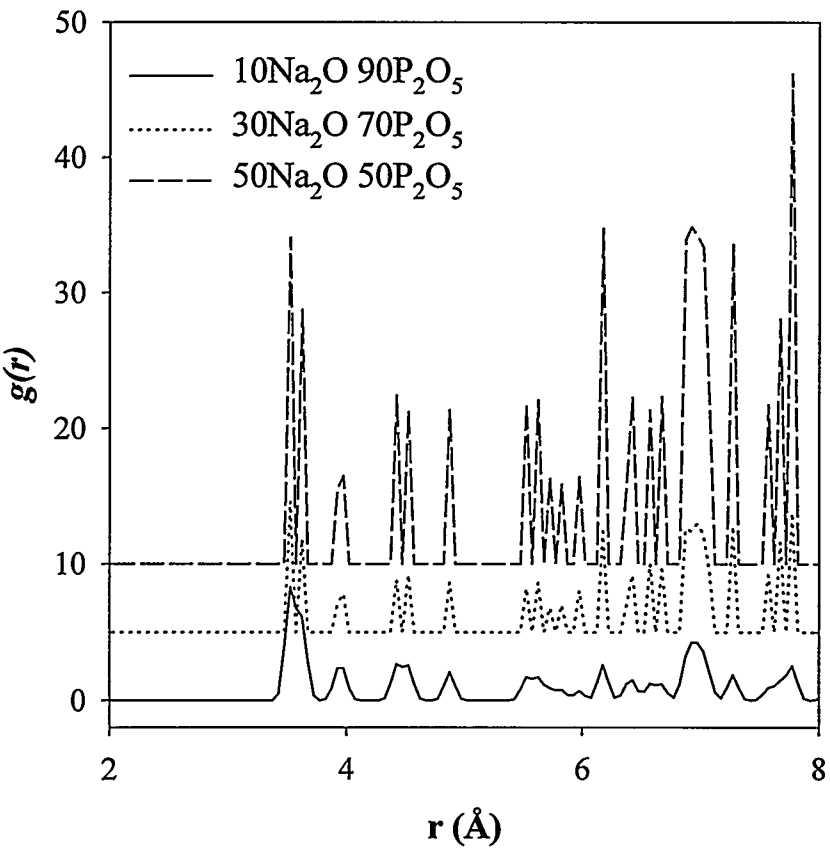

Alam et al Fig 4

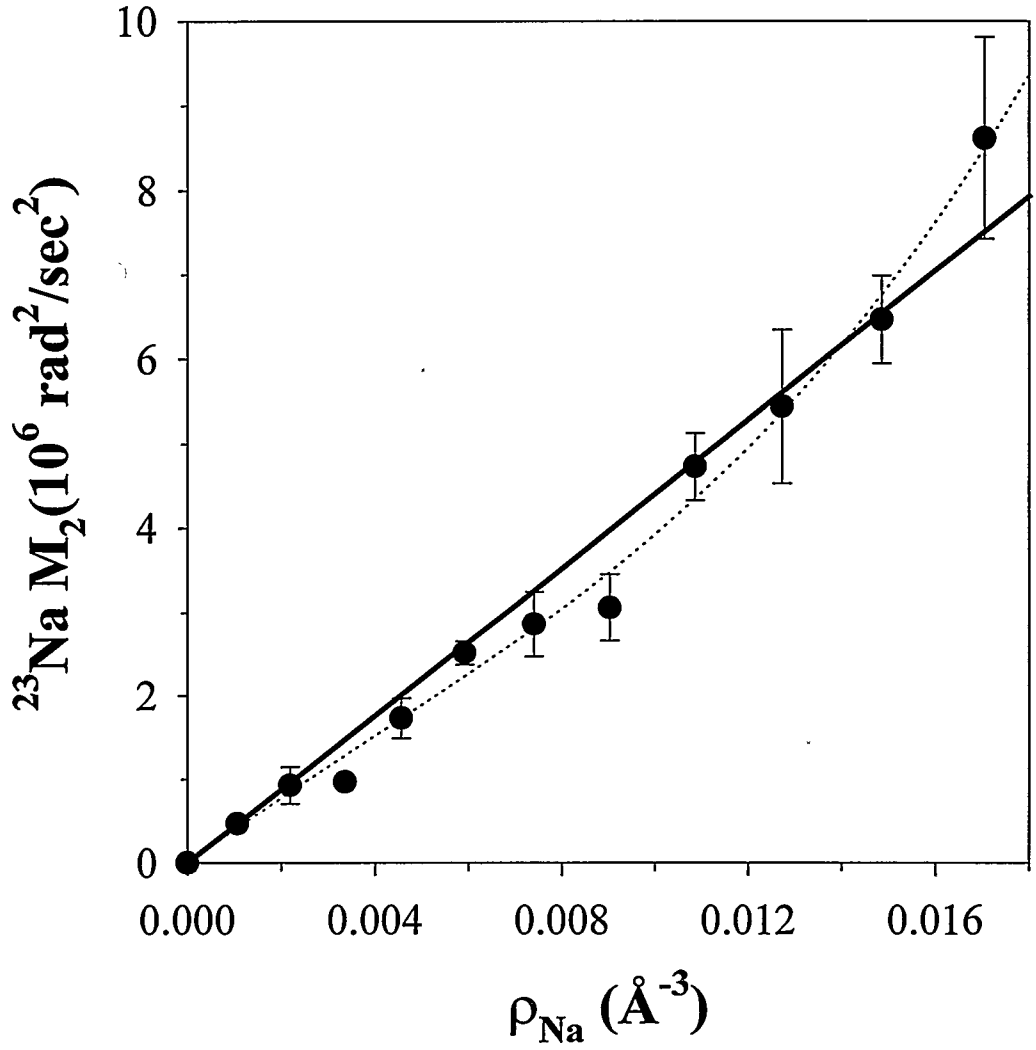

Alam et al Fig 5

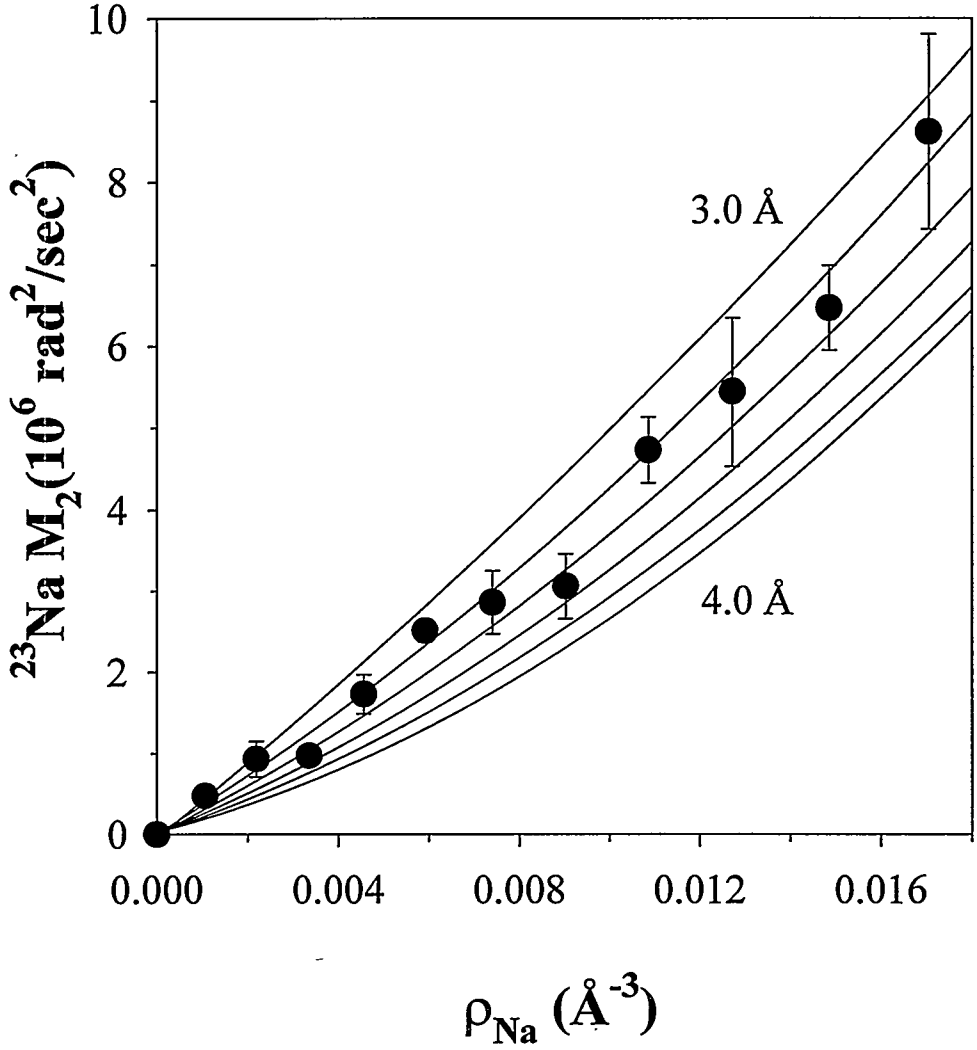

Alam et al. Fig. 6

Alam et al. Fig. 7

a)

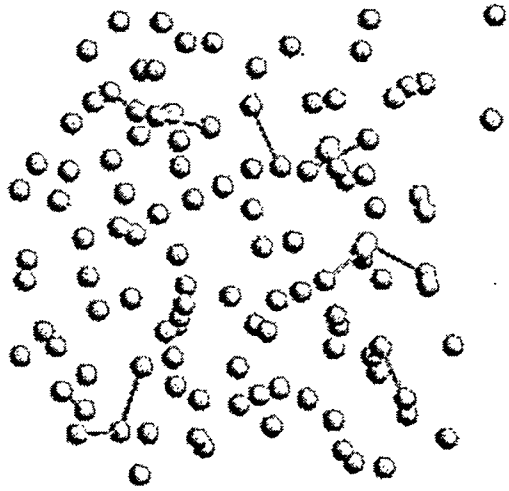

b)

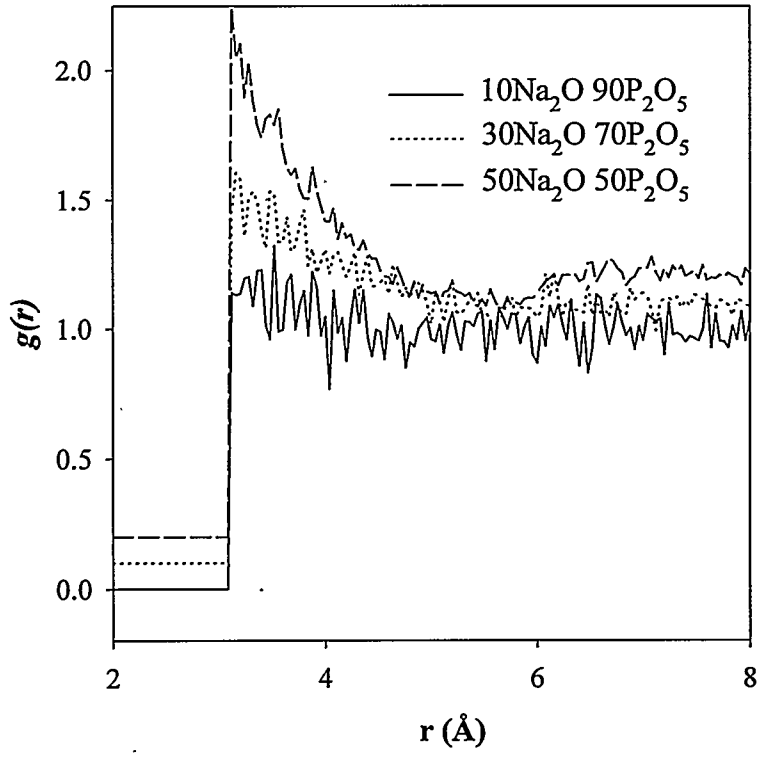

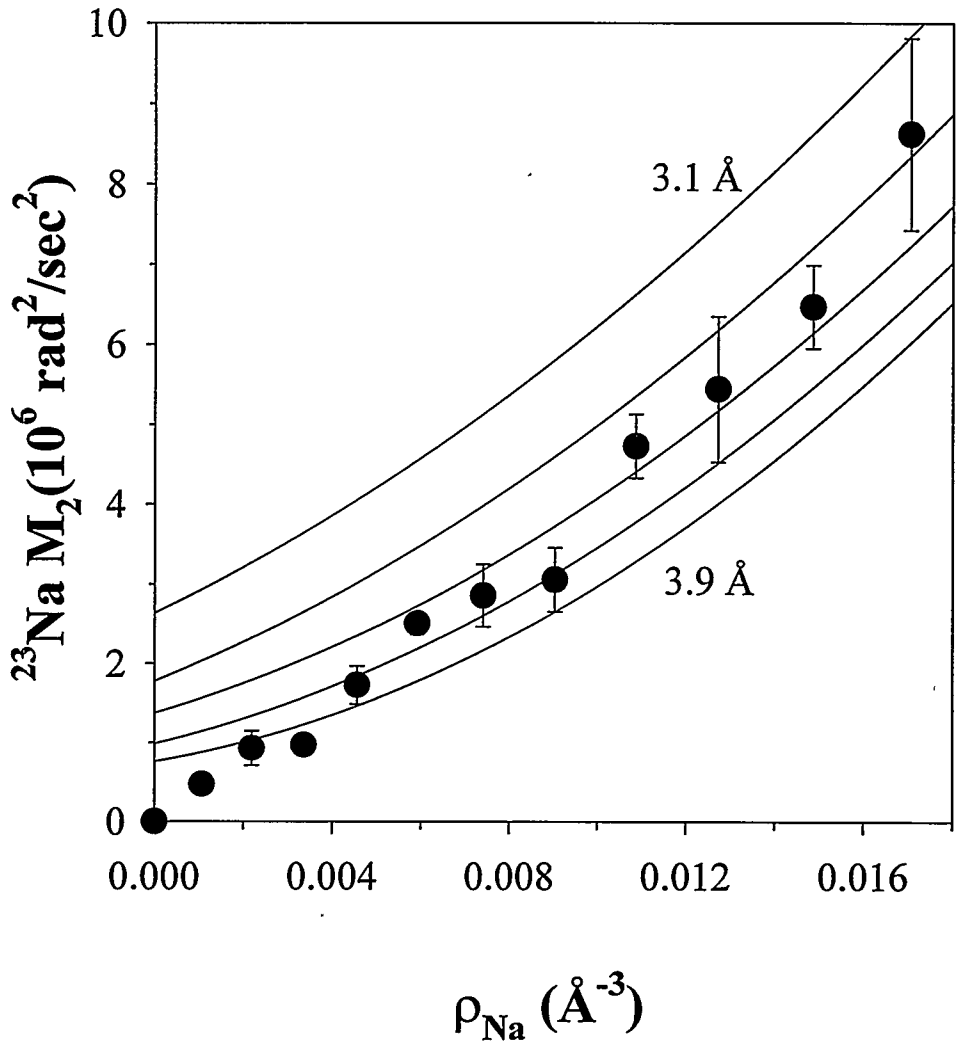

Alam et al. Fig. 8

Alam et al. Fig 9

a)

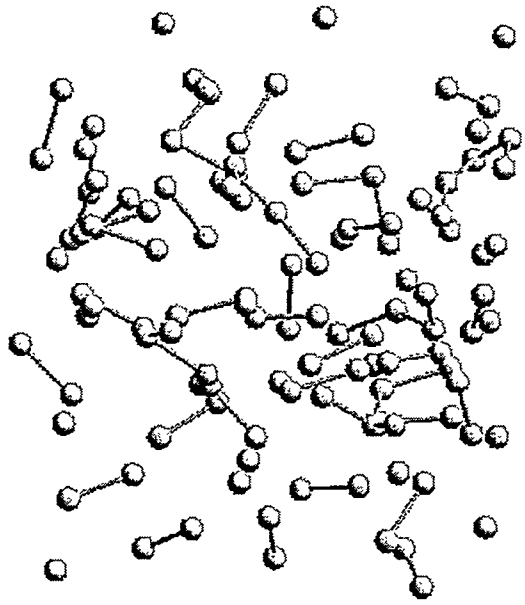

b)